Improved control for DFIG based wind power system under voltage dips using ADRC optimized by genetic algorithms

Original Scientific Paper

Noureddine Elmouhi
Mohammed V University in Rabat,
Ecole Nationale Supérieure d'Arts et Métiers (ENSAM),
Research Center in Sciences and Technologies of Engineering and Health (STIS)
Institut supérieur d'ingénierie et des affaires (ISGA Rabat),
Laboratory of Innovation in Management and Engineering for Enterprise (LIMIE), Rabat, Morocco.
n.elmouhi@gmail.com

Ahmed Essadki
Mohammed V University in Rabat,
Ecole Nationale Supérieure d'Arts et Métiers (ENSAM),
Research Center in Sciences and Technologies of Engineering and Health (STIS), Rabat, Morocco
Ahmed.essadki1@gmail.com

Hind Elaimani
Mohammed V University in Rabat,
Ecole Nationale Supérieure d'Arts et Métiers (ENSAM),
Research Center in Sciences and Technologies of Engineering and Health (STIS)
Institut supérieur d'ingénierie et des affaires (ISGA Rabat),
Laboratory of Innovation in Management and Engineering for Enterprise (LIMIE), Rabat, Morocco.
h.elaimani@gmail.com

Abstract *– Many countries have focused on the study of the electrical energy production using wind generators. These studies include maintaining the production under disturbed conditions at the grid connection point of wind farms, and maintaining production during voltage dips. Electrical grid operators have established different requirements for connecting renewable energy production systems to electrical grids. In this research paper, we are interested in the study of the wind power system based on the Doubly Fed Induction Generator during a voltage dip. We are also developing a control approach based on Active Disturbance Rejection Control and Genetic Algorithms, which aims to control the stator flux variations which should be taken into account during the current controllers computing. This control strategy will allow the wind power system to remain connected to the grid under voltage dips, and to resume the normal operation after the fault disappearance. The model of the wind power system and the proposed control strategy, are tested in the MATLAB-Simulink software.*

Keywords*: ADRC, DFIG Control, wind turbine, MPPT, wind energy, genetic algorithm, voltage dips*

1. INTRODUCTION

In wind turbine-based power generation stations, the Doubly-fed Induction Generator (DFIG) is the most adopted and installed configuration by leaders in wind turbine construction around the world. Indeed, it has many advantages due to its ability to supply energy at constant voltage and frequency for a variable rotor speed, which allows maximum power extraction regardless of the wind speed [1], [2].

The configuration of wind power system based on DFIG is presented in figure 1. As shown in this structure, the stator is directly connected to the grid and the rotor is connected by means of two converters, a grid filter and a transformer [2,3,4].

The electrical energy produced must correspond to the expectations of consumers, producers and grid managers. Among the main criteria for measuring the level of the energy produced quality, we find the sensitivity to voltage dips and the quality of the injected signal (harmonic distortion rate).

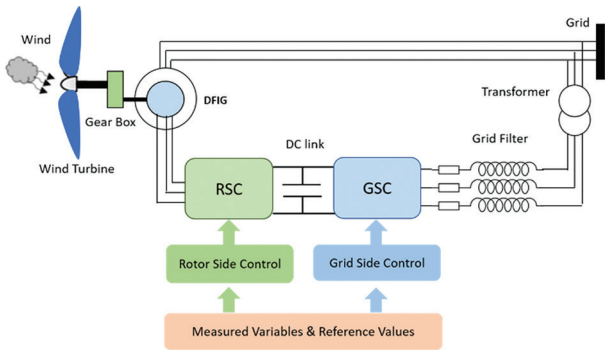

Fig. 1. Variable speed wind turbine structure

The DFIG presents many difficulties with regard to compliance with the conditions for connection to the electricity grid imposed by the electrical grid managers. Indeed, it is very sensitive to electrical faults, in particular voltage dips in the grid [5]. During voltage faults, the wind power system is destabilized and the internal protection system intervenes to its disconnection from the grid. This disconnection reinforces the imbalance in voltage and frequency. However, wind turbines are forced to remain connected after voltage dips [3,4].

The use of the DFIG is based on the power converters as an interface with the grid, this interface generates harmonic currents liable to induce harmonic voltages in the grid, which requires the limitation of these harmonic currents.

For the problem related to voltage dips, some research [6,7,8] has proposed an approach which is based on PI controllers for the command adaptation in the voltage dips event. However, this solution does not present the robustness against the internal parameters change of the DFIG. Especially since the synthesis of these regulators is based on these parameters.

Other authors, in other works [9,10], has proposed to use synchronous static compensators to participate in voltage setting during voltage dips. The problem of this solution is that it presents a very high implementation cost.

The authors in [11] propose a method for better attenuation of switching harmonics. This method is based on linear Active Disturbances Rejection Control ADRC while providing compensation of resonant poles in the LCL filter via zero pole cancellation [11]. This strategy is effective under the grid impedance uncertainty, and ensures the filtering of the parameter's uncertainties without adjustment of control. This approach has shown good performance compared to control by conventional PI regulators.

In [12] and [13], the work is focused on the use of an LCL filter and the problem of interactive resonance which is triggered by the interaction between inverters, this causes a mutual current in the grid. For this disturbance, considered as external, the authors propose a control approach to estimate and then cancel these disturbances by using ADRC technique [12]. This technique is introduced first for an L filter and then for an LCL. The results of this approach showed that the resonance and antiresonance peaks present in the LCL filter, with the current on the inverter side, are damped using the pole-zero cancellation technique [13].

In this paper, the work is focused on the study and the analysis of the DFIG behavior in the case of the first criterion relating to the electrical energy quality, mentioned above, which is the sensitivity to voltage dips. In effect, the drop in stator voltage leads to:

- A decrease in the electromagnetic torque which causes an increase in the speed of rotation.
- A drop in the magnetic flux and consequently the demagnetization of the machine.
- An increase in the stator and rotor current as well as the DC link voltage. This increase triggers the protection circuits and consequently the wind turbine disconnection.

The objective is to establish a robust control method using ADRC and genetic algorithms, which allows to keep the wind turbine connected to the grid. Indeed, the ADRC, with the proposed adaptation in this paper, makes it possible to resume normal operation after the fault disappearance, while ensuring robustness against changes in the internal parameters system. The genetic algorithm makes it possible to find an optimal adjustment of the different controllers used in this approach.

This article is structured as follows: the first part will be devoted to the development of the dynamic model of the wind power system, then we will develop the Active Disturbance Rejection Control of converters. The second part will be entirely devoted to the study of the system behavior during the voltage fault, and to the adaptation of the DFIG command. The final section of this paper will be devoted to presenting and interpreting simulation results using the MATLAB / Simulink environment.

2. DYNAMIC MODEL OF WIND POWER SYSTEM

2.1. WIND TURBINE MODEL

A wind turbine is characterized by an aerodynamic torque, which is given by the following expression [10]:

$$T_{aer} = \frac{P_{extr}}{\Omega_t} = \frac{1}{2.\Omega_t} \rho \, \pi \, R^2 \, v^3 C_p(\beta, \lambda) \tag{1}$$

P_{extr} is the maximum power that can be extracted which is given by [3,14]:

$$P_{extr} = \frac{1}{2} \rho \, \pi \, R^2 \, v^3 C_p(\beta, \lambda) \tag{2}$$

C_p is a power coefficient turbine, which depends on λ, the velocity ratio, and the pich angle β [3]. It is expressed by:

$$C_p(\lambda, \beta) = \frac{1}{2}\left(116\left(\frac{1}{\lambda+0.08\beta} + \frac{0.035}{1+\beta^3}\right) - 0.4\beta - 5\right) e^{-21\left(\frac{1}{\lambda+0.08\beta} + \frac{0.035}{1+\beta^3}\right)} + 0.0068\lambda \tag{3}$$

The mechanical speed is expressed by the following expression [3,15]:

$$J.\frac{d\Omega_{mec}}{dt} = T_{mec} \tag{4}$$

$$J = \frac{J_{Turbine}}{G^2} + J_g \tag{5}$$

$$J\frac{d\Omega_{mec}}{dt} + f\Omega_{mec} = T_g - T_{em} \tag{6}$$

2.2. DFIG MODELLING

The equations of DFIG model in the Park reference dq and the electromagnetic torque are given by the following expressions [16]:

$$\begin{cases} \Phi_{sd} = L_s i_{sd} + L_m i_{rd} \\ \Phi_{sq} = L_s i_{sq} + L_m i_{rq} \\ \Phi_{rd} = L_r i_{rd} + L_m i_{sd} \\ \Phi_{rq} = L_r i_{rq} + L_m i_{sq} \end{cases} \tag{7}$$

$$\begin{cases} V_{sd} = R_s i_{sd} + \frac{d\Phi_{sd}}{dt} - \omega_s \Phi_{sq} \\ V_{sq} = R_s i_{sq} + \frac{d\varphi_{sq}}{dt} + \omega_s \Phi_{sd} \\ V_{rd} = R_r i_{rd} + \frac{d\varphi_{rd}}{dt} - \omega_r \Phi_{rq} \\ V_{rq} = R_r i_{rq} + \frac{d\varphi_{rq}}{dt} + \omega_r \Phi_{rd} \end{cases} \tag{8}$$

$$T_{em} = p\frac{L_m}{L_s}(i_{rd}\Phi_{sq} - i_{rq}\Phi_{sd}) \tag{9}$$

The expressions of active and reactive powers are:

$$\begin{cases} P_s = V_{sd} i_{sd} + V_{sq} i_{sq} \\ Q_s = V_{sq} i_{sd} - V_{sd} i_{sq} \end{cases} \tag{10}$$

$$\begin{cases} P_r = V_{rd} i_{rd} + V_{rq} i_{rq} \\ Q_r = V_{rq} i_{rd} - V_{rd} i_{rq} \end{cases} \tag{11}$$

For a medium and high power DFIG, the stator resistance Rs can be neglected [17]. The previous equations can be simplified by directing the stator flux in accordance with d-axis:

$$T_{em} = -\frac{3}{2}p\frac{L_m}{L_s} i_{rq}\Phi_s \tag{12}$$

$$P_s = -V_{sq}\frac{L_m}{L_s} i_{rq} \tag{13}$$

$$Q_s = -\frac{V_{sq}\Phi_s}{L_s} - V_{sq}\frac{L_m}{L_s} i_{rd} \tag{14}$$

2.3. POWER CONVERTERS

The connection of the DFIG to the grid is made through a converter connected to the rotor, and a converter linked to the grid with a grid filter and transformer [14,15,18,19]. This structure is shown in figure 2:

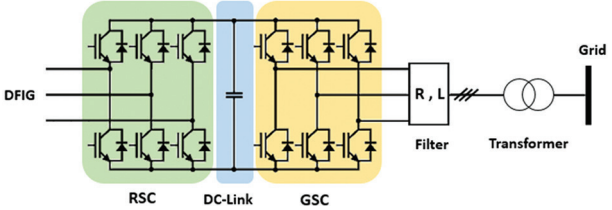

Fig. 2. Bloc diagram of RSC, DC link and GSC

The RSC ensures the active and reactive powers control so that they follow their references, and the GSC controls the DC link voltage [20].

3. ACTIVE DISTURBANCE REJECTION CONTROL STRATEGY

The Active disturbances rejection control is a robust command based on the extension of the model system by a use of a «Extended State Observer (ESO)» to estimate and cancels internal and external disturbances [3,4,8,21]. Figure 3 and 4 shows the basic structure of ADRC controller and the ESO [22]:

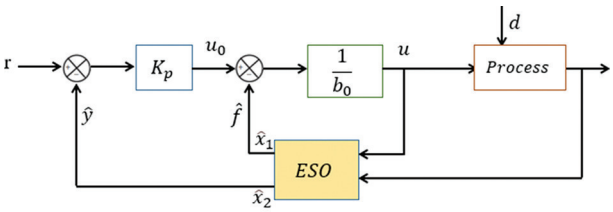

Fig. 3. Structure of the first-order ADRC controller

The extended state observer gains are theoretically defined by [23] : $\beta_1=2\omega_0$ *and* $\beta_1=\omega_0^2$

Where ω_0 is determined as a function of the closed-loop system poles to ensure both fast observer dynamics and minimal sensitivity to noise.

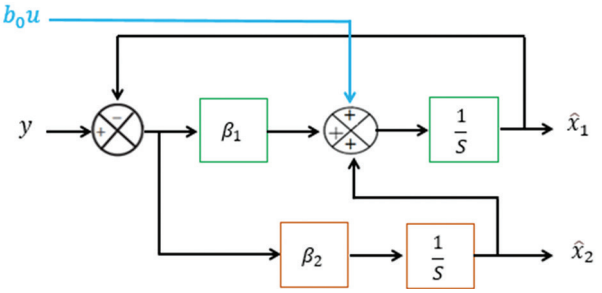

Fig. 4. Extended State Observer ESO

3.1. ROTOR SIDE CONVERTER CONTROL RSC

By adopting the assumptions relating to the choice of the park reference and to the stator resistance, the rotor currents expressions can be rearranged to be in the following form [24]:

$$\frac{di_{rd}}{dt} = -\frac{R_r}{\sigma L_r} i_{rd} + \omega_r . i_{rq} + \frac{1}{\sigma L_r} V_{rd} \tag{15}$$

$$\frac{di_{rq}}{dt} = -\frac{R_r}{\sigma L_r} i_{rq} - \omega_r . i_{rd} - \omega_r \frac{L_m}{\sigma L_r L_s}\Phi_s + \frac{1}{\sigma L_r} V_{rq} \tag{16}$$

Where $\sigma = 1 - \frac{L_m^2}{L_s L_r}$ represent the dispersion coefficient. We put these expressions in the following form:

$$\frac{di_{rd}}{dt} = f_d(i_{rd}, d, t) + b_0 u(t) \tag{17}$$

$$\frac{di_{rq}}{dt} = f_q(i_{rq}, d, t) + b_0 u(t) \tag{18}$$

Where:

$$\begin{cases} f_d = -\frac{R_r}{\sigma L_r} i_{rd} + \omega_r . i_{rq} + (\frac{1}{\sigma L_r} - b_0) V_{rd} \\ u = V_{rd} \quad , \quad b_0 = \frac{1}{\sigma L_r} \end{cases} \tag{19}$$

$$\begin{cases} f_{dq} = -\frac{R_r}{\sigma L_r} i_{rq} - \omega_r . i_{rd} - \omega_r \frac{L_m}{\sigma L_r L_s} \Phi_s + (\frac{1}{\sigma L_r} - b_0) V_{rq} \\ u = V_{rq} \quad , \quad b_0 = \frac{1}{\sigma L_r} \end{cases} \tag{20}$$

f_d and f_q represent the disturbances impacting respectively affecting the direct and quadratic rotor currents. Vrd and Vrq represent the control set points of the current's loops. The gain parameter b0 represent the known part of the system parameters [24]. It is opted as:

$$b_0 = \frac{1}{\sigma L_r}$$

The reference current i_{rqRef} makes it possible to regulate the electromagnetic torque to its imposed reference by the maximum power point tracker (MPPT) bloc [24]. Its expression is given by the equation 21:

$$i_{rqRef} = \frac{-2L_s}{pL_m \Phi_{sq}} T_{emRef} \tag{21}$$

The reference rotor current i_{rdRef} is determined in order to control the reactive power provided or absorbed by the DFIG [15,25]. Its expression is given by the equation 22. The diagram of the RSC is presented in figure 5.

$$i_{rdRef} = \frac{\Phi_s}{L_m} - \frac{L_m}{V_s L_m} Q_{sref} \tag{22}$$

The parameters K_p, β_1 and β_2 of the ADRC controllers are determined so that the rotor currents follow their reference i_{rqRef} and i_{rdRef} [26]. This is obtained using genetic algorithms which make it possible to have an optimum response.

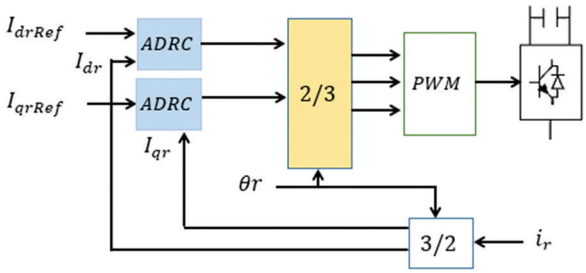

Fig. 5. Block diagram of the RSC

3.2. CONTROL OF GSC

The grid filter currents i_{qf} and i_{df} are given by the following expressions [27]:

$$\frac{di_{df}}{dt} = \frac{1}{L_f} V_{sd} - \frac{R_f}{L_f} i_{df} - w_s i_{qf} - \frac{1}{L_f} V_{df} \tag{23}$$

$$\frac{di_{qf}}{dt} = \frac{1}{L_f} V_{sq} - \frac{R_f}{L_f} i_{qf} - w_s i_{df} - \frac{1}{L_f} V_{qf} \tag{24}$$

According to the ADRC structure, these expressions can be rearranged to be in the following form:

$$\frac{di_{df}}{dt} = f_{df}(i_{df}, d, t) + b_0 u(t) \tag{25}$$

Where:

$$\begin{cases} f_{df} = \frac{1}{L_f} V_{sd} - \frac{R_f}{L_f} i_{df} - w_s i_{qf} + (\frac{1}{L_f} - b_0) V_{df} \\ u = V_{df} \quad , \quad b_0 = -\frac{1}{L_f} \end{cases} \tag{26}$$

$$\frac{di_{qf}}{dt} = f_{qf}(i_{qf}, d, t) + b_0 u(t) \tag{27}$$

Where:

$$\begin{cases} f_{qf} = \frac{1}{L_f} V_{sq} - \frac{R_f}{L_f} i_{qf} - w_s i_{df} + (\frac{1}{L_f} - b_0) V_{qf} \\ u = V_{qf} \quad , \quad b_0 = -\frac{1}{L_f} \end{cases} \tag{28}$$

The *iqf* and *idf* currents can follow their references by making a good adjustment of the ADRC controller parameters. The gain parameter b0 is opted as:

$$b_0 = -\frac{1}{L_f}$$

The block diagram of the GSC is given in figure 6:

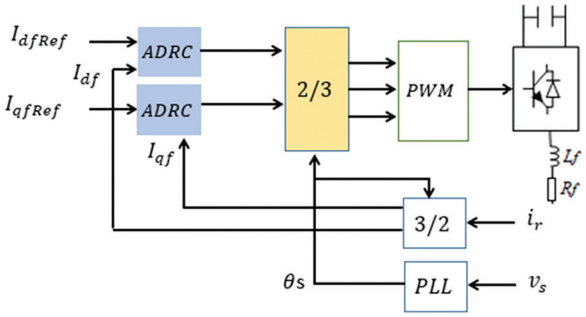

Fig. 6. Diagram for the GSC

4. CONTROL STRATEGY OF DFIG DURING A VOLTAGE DIP

During a voltage dip, the electromagnetic torque of the generator decreases, which leads to an increase in the rotation speed. This increase is more important as the voltage dip is deeper [20,28]. The stator is directly connected to the grid, which causes the stator flux decrease. When the fault disappears, the DFIG risks re-magnetizing itself suddenly, which causes a strong current to be drawn in and subsequently a system disconnection [25]. However, the dynamics of the stator flux should not be neglected during sizing of the current controller.

The voltage dip also provokes an increase in stator current. This high current passes through the rotor and the converters on the rotor side [22,29]. Which also leads to an increase in the DC-link voltage and consequently the destruction of the power converters [30,31].

The concern during the voltage dip is to keep the wind turbine connected during the fault and to ensure a restart after the disappearance fault. We are also interested to keep the electrical and mechanical quantities of the system under the threshold values trigger-

ing the protection systems [4,32]. Without neglecting the flux dynamics stator flux.

The proposed method to keep the wind turbine connected, consists in taking into account the stator flux variations, during the generation of the command voltages V_{rd} and V_{rq}, which are necessary for the rotor side control. Consequently, the neglected terms in the ADRC control equations without voltage dips must be taken into account, and the expressions of the control quantities must be recalculated, as well as the structure of the ADRC control which must be adapted.

The stator currents are given from equation 8:

$$i_{sd} = \frac{\Phi_{sd} - L_m i_{rd}}{L_s} \quad (29)$$

$$i_{sq} = \frac{\Phi_{sq} - L_m i_{rq}}{L_s} \quad (30)$$

From equation 9, the rotor flux is given by:

$$\varphi_{rd} = \sigma L_r i_{rd} + \frac{L_m}{L_s}\Phi_{sd} \quad (31)$$

$$\varphi_{rq} = \sigma L_r i_{rq} + \frac{L_m}{L_s}\Phi_{sq} \quad (32)$$

From the previous equations, the stator voltages can be given by the following expressions:

$$V_{sd} = \frac{R_s}{L_s}\Phi_{sd} - \frac{R_s}{L_s} i_{rd} + \frac{d\Phi_{sd}}{dt} \quad (33)$$

$$V_{sd} = \frac{R_s}{L_s}\Phi_{sd} - \frac{R_s}{L_s} i_{rd} + \frac{d\Phi_{sd}}{dt}$$

So, by replacing the flux expressions in the rotor voltages expressions, we obtain:

$$V_{rd} = R_r i_{rd} + \sigma L_r \frac{di_{rd}}{dt} - \omega_r \sigma L_r i_{rq} - \omega_r \frac{L_m}{L_s}\Phi_{sq} + \frac{L_m}{L_s}\frac{d\Phi_{sd}}{dt}$$
$$V_{rq} = R_r i_{rq} + \sigma L_r \frac{di_{rq}}{dt} + \omega_r \sigma L_r i_{rd} + \omega_r \frac{L_m}{L_s}\Phi_{sd} + \frac{L_m}{L_s}\frac{d\Phi_{sq}}{dt} \quad (34)$$

$$V_{rd} = R_r i_{rd} + \sigma L_r \frac{di_{rd}}{dt} + e_q + e_{\Phi_d}$$

$$V_{rq} = R_r i_{rq} + \sigma L_r \frac{di_{rq}}{dt} + + e_d + e_{\Phi_q}$$

Where:

$$e_d = \omega_r \sigma L_r i_{rd}$$
$$e_q = -\omega_r \sigma L_r i_{rq}$$
$$e_{\Phi_d} = \frac{L_m}{L_s}\left(-\omega_r \Phi_{sq} + \frac{d\Phi_{sd}}{dt}\right)$$
$$e_{\Phi_q} = \frac{L_m}{L_s}\left(\omega_r \Phi_{sd} + \frac{d\Phi_{sq}}{dt}\right)$$

We can so present a DFIG control block by ADRC adapted in the voltage dip event (figure 7):

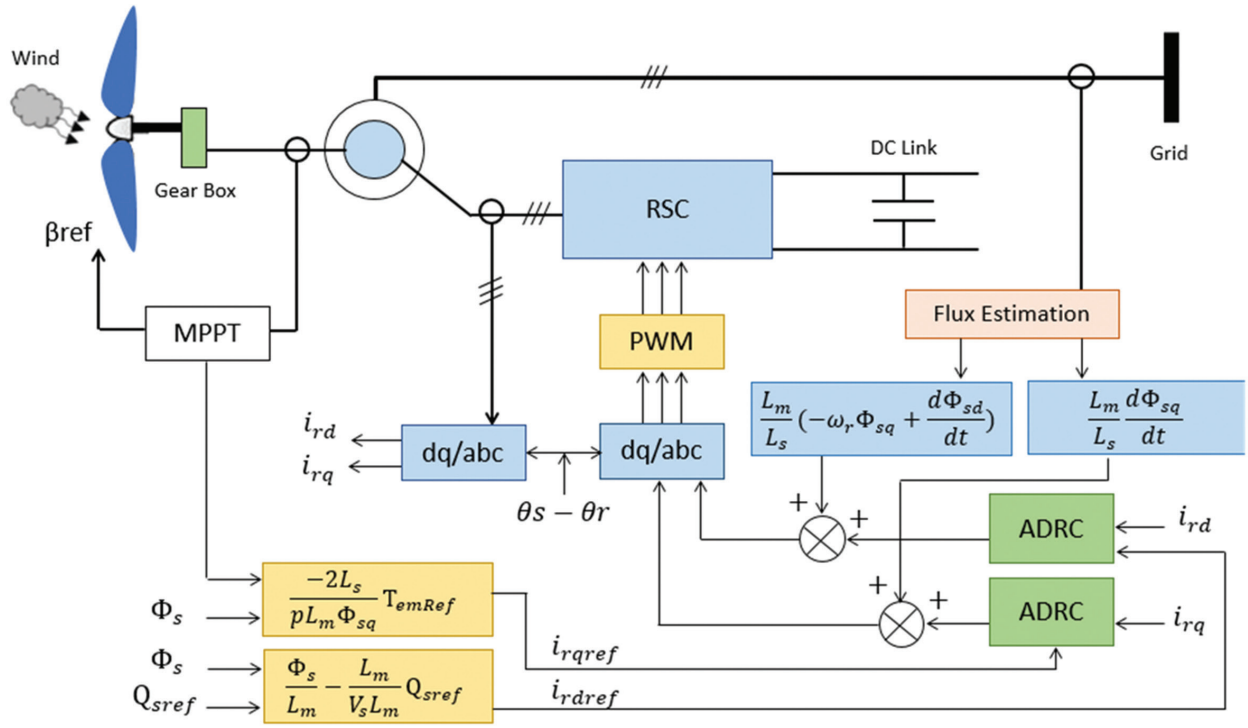

Fig. 7. Block diagram of DFIG control in the voltage dip event

The proposed method, which consists in taking into account the dynamics of the stator flux during a voltage dip, can be further improved by using an LCL filter instead of an L filter. Indeed, the results presented by the authors in [11-13] show that this higher order filter allows a better attenuation and reduction of the current harmonics absorbed by the power converters. The resonance effect in this filter will be damped using zero pole cancellation. This allows to keep preserved dynamic performance and a higher stability margins.

5. GENETIC ALGORITHM

The genetic algorithm GA is an optimization method based on theories of natural selection [9]. In the litera-

ture, this technique is recognized to be very effective and efficient in finding optimal solutions to optimization problems. It makes it possible to avoid local minima constituting a major problem in the case of nonlinear systems [33,34].

In this technique, the solutions to an optimization problem are represented as chromosomes from an initial population to evolve to an optimal solution with repeated modification [34].

The application of the algorithm is done in three stages: selection, crossing and mutation. these three steps are applied to create new individuals and subsequently assess their performance against the previous ones using a fitness function. [34].

To have the optimal solution, represented by the best individuals, this algorithm must be repeated for many generations and finally stops when it reaches these chromosomes [34]. In figure 8, we present the genetic algorithm optimization diagram to be established to have the ADRC controllers' parameters.

In our case, genetic algorithm is used to optimize the DFIG control in the voltage dip event. the procedure used is as follows:

For each individual belonging to the real population, the objective function is calculated. Therefore, the parameters of the ADRC controller can be decoded, and then the DFIG model is simulated to obtain the objective function value.

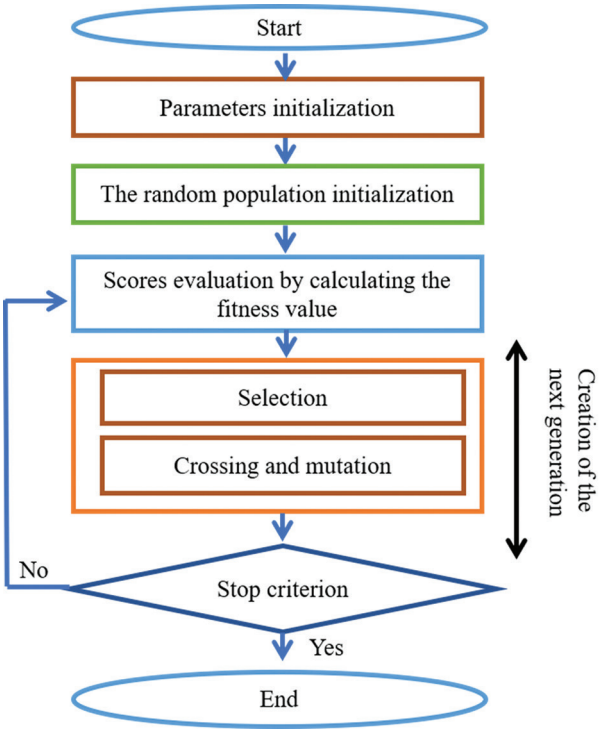

Fig. 8. Genetic Algorithm optimization diagram

In our case, genetic algorithm is used to optimize the DFIG control in the voltage dip event. the procedure used is as follows:

For each individual belonging to the real population, the objective function is calculated. Therefore, the parameters of the ADRC controller can be decoded, and then the DFIG model is simulated to obtain the objective function value.

The following population is generated based on the operators of the genetic algorithm, namely selection, crossing and mutation. These two steps are repeated from generation to generation until a final population with optimal values is obtained.

This algorithm is used in our case to adjust the parameters K_p, β_1 and β_2 so as to obtain the optimal performance in terms of dynamics, robustness and disturbance rejection. The objective function is chosen so that the difference between the reference power and the measured power is as small as possible.

The types of the GA operations used in this work, and the parameters' initialization are listed in Table 1 and 2 below:

Table 1. Types of the GA operations used

Property	Type
Selection	GA default selection function
Mutation	Uniform
Crossover	Arithmetic

Table 2. Genetic algorithm parameters

Property	Value	
	Backstepping	ADRC
Number of variables	2	3
Population size	50	50
Maximum number of generations	500	500
Mutation fraction	0.01	0.01
Crossover fraction	0.08	0.08
Tolerance	500	500

The best score value and mean score versus generation for the ADRC method are represented in the following figure (figure 13):

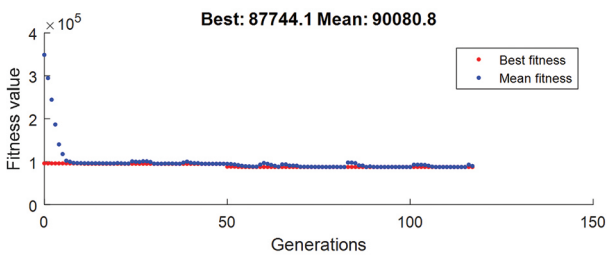

Fig. 9. ADRC Fitness value

Using the previous optimization diagram, the Parameters' evolution during the generation is presented in figure 10 and their values obtained bay GA are listed in table 3:

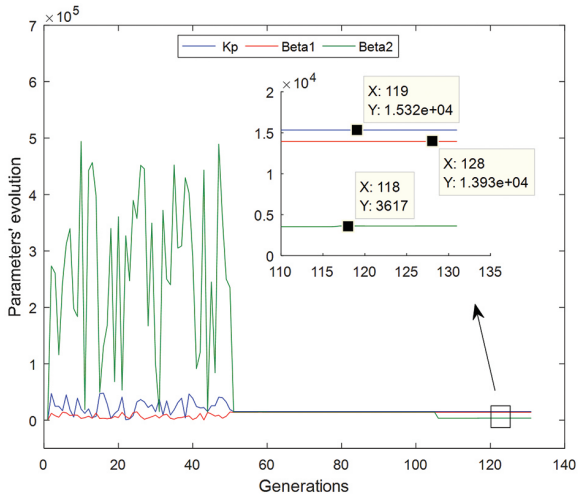

Fig. 10. Parameters' evolution during the generation

Table 3. ADRC controller parameters

Parameter	Symbol	Value
Currents controller gain	k_p	15320
Extended state observer gains	β_1	13930
	β_2	3617

6. SIMULATION RESULTS

To study the DFIG behavior in the voltage dip event and the performance of the proposed strategy, we consider a voltage dip with a depth of 50% that lasts 600ms.

The duration of the considered voltage dip is relatively short compared to the wind speed variations and fluctuations. Therefore, we can study with a constant wind speed equal to 12 m.s-1. The DFIG parameters as well as the parameters of DC link and filter are summarized in table 4 and table 5 in appendix. Immediately after the fault appears at t = 1s, the generator voltage drops, as shown in figure 11:

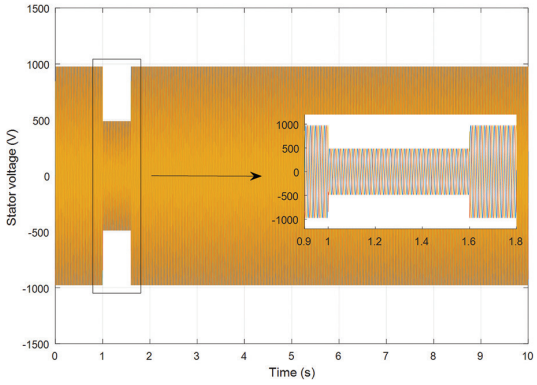

Fig. 11. Stator voltages

In next figures, 12 and 13, we present the stator currents with the conventional method and the adapted control strategy.

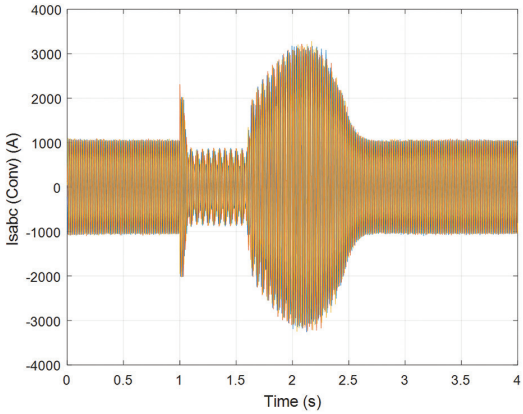

Fig. 12. Stator currents with the conventional strategy

From these two figures, we notice that by taking into account the stator flux dynamics, the modified control strategy generates less oscillations compared to the classical method which presents large oscillations and an unbalance after the fault disappearance. The current peak, that occurs when the voltage dip occurs, is due to the additional power introduced into the system during the drop of the transmitted power to the grid. Therefore, the protection circuits responsible for disconnecting the wind turbine from the grid will not be triggered. the system can therefore resume normal operation after the fault disappearance

In figure 14, we present the stator active power transferred to the grid. When the fault occurs, it can be noted that, in the classical method, the active power is completely cancelled out and shows a very remarkable additional overshoot after the fault disappears. This is due to the instability in the torque evolution and the rotation speed, which leads to the disconnection of the turbine by the internal protection systems. In the case of the modified strategy, this power is non-zero during the fault, which shows that the proposed method allows the generator magnetization during the voltage dip. The generation of active power resumes after the fault disappears and recapture its initial value, without exhibiting many oscillations or a large overshoot of the reference value which causes the activation of the protection circuits.

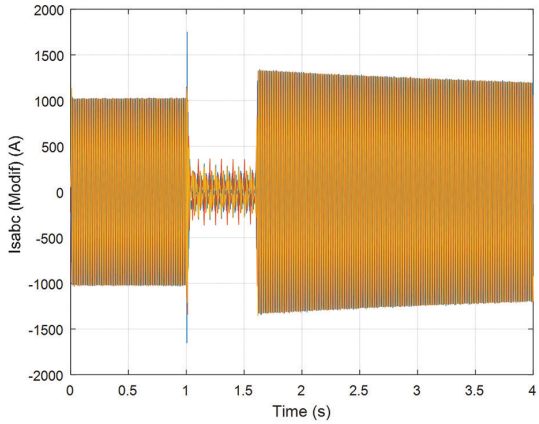

Fig. 13. The stator currents with the modified strategy

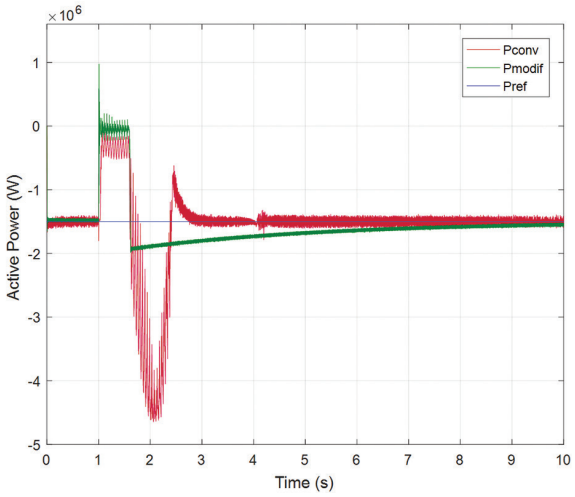

Fig. 14. Active stator power

Figure 15 shows the evolution of the stator reactive power. This power must be normally null to ensure a unitary power factor. When the fault occurs, for the proposed strategy, we note that this power presents some oscillations during a transient state and returns to its value after the fault. In the case of the conventional method, this power is not zero during the fault and presents a large overshoot after the fault disappearance.

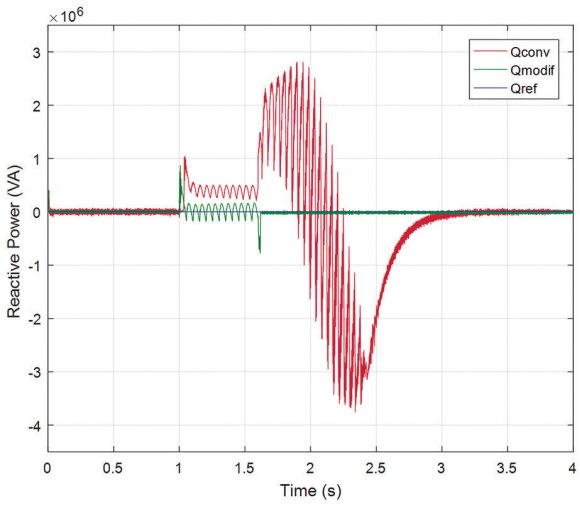

Fig. 15. Reactive stator power

In Figures 16 and 17, we present the rotor currents before, during and after the voltage dip. From these figures, we notice that these currents increase after the appearance of the fault. A high rotor current can damage the rotor side converter, which can be avoided by protecting with an additional circuit called Crowbar. Its role is to limit the rotor current and the DC link voltage.

From these figures it can be seen that in the case of the conventional control method, the currents are completely disturbed after the appearance of the voltage dip and present an imbalance after the fault. For the modified strategy, the currents return more quickly to their normal values before the fault appearance without remarkable overshoot.

It can therefore be noted that the proposed approach makes it possible to improve the DFIG behavior during a voltage dip, by limiting the stator and rotor currents, consequently keeping the wind turbine connected after the fault disappearance.

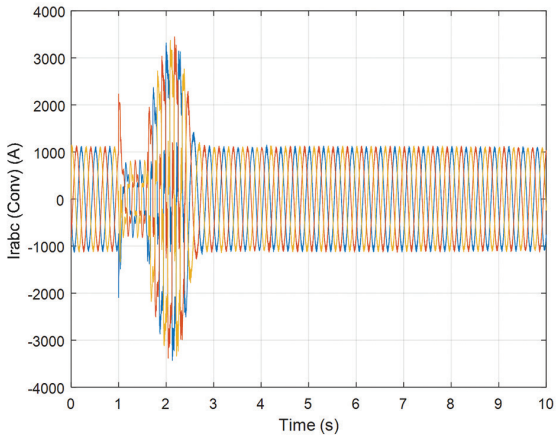

Fig. 16. Rotor currents with the conventional strategy

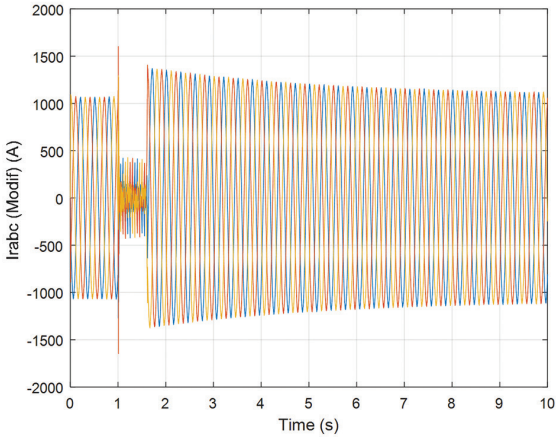

Fig. 17. Rotor currents with the modified strategy

7. CONCLUSION

In this research paper, we have dealt with the dynamic modeling and control of the wind energy conversion system based on DFIG, using active disturbance rejection control. We are interested in evaluating the dynamic performances of this system in the voltage dip event, and in developing a modified control strategy, which makes it possible to keep the DFIG connected to the power grid during this fault.

The voltage dip causes the stator flux decrease. To ensure the magnetization of the generator during and after the voltage dip, the stator flux dynamics must not be neglected and must be considered in the controller computing.

The simulation results were presented to ensure the validity and performance of the proposed control strategy based on ADRC and genetic algorithms, which allowed the production system to stay connected during the voltage dip and regain it's the normal operation after the fault has disappeared.

As a perspective, the quality of the generated power can be further improved by integrating a higher order link filter, with an eliminating method of the resonance effect. This will eliminate harmonic distortion in the currents. We can also focus the study on the impact of the uncertainty of the grid impedance on the control performances.

8. NOMENCLATURE

- R turbine radius
- ρ Air density
- v Wind speed
- Ω_t Turbine speed
- C_p Power coefficient
- λ Velocity ratio
- β Pich angle
- J Total inertia
- $J_{Turbine}$ Turbine inertia
- J_g Generator inertia
- f Coefficient of viscous friction
- G Gain multiplier
- Φ_{sdq} dq axis Stator fluxes
- Φ_{rdq} Rotor fluxes
- V_{sdq} Stator voltages according to dq axis
- V_{rdq} Rotor voltages according to dq axis
- i_{sdq} Stator currents according to dq axis
- i_{rdq} Rotor currents according to dq axis
- ω_s Rotor angular frequency
- ω_r Stator angular frequency

9. APPENDIX

Table 4. DFIG Parameters

Parameter	Symbol	Value
Rated power	P_s	1.5 M
Stator resistance	R_s	8.9 mΩ
Rotor resistance	R_r	13.7 mΩ
Stator inductance	L_s	13.7 mH
Rotor inductance	L_r	13.67 mH
Mutual cyclic inductance	L_m	13.5 mH
Number of pole pairs	p	2
Optimal tip speed ratio	λ_{opt}	8.1
Maximal power coefficient	C_{pmax}	0.48

Table 5. Parameters of the RL filter and the DC bus

Parameter	Symbol	Value
Filter resistance	R_t	0.25 Ω
Filter inductance	L_t	0.005 H
DC link Capacitor	C	0.0044 F
DC link voltage	U_{dc}	1200 V

10.REFERENCES:

[1] I. Kharchouf, A. Essadki, M. Arbaoui, T. Nasser, "Modeling and PI Control Strategy of DFIG Based Wind Energy Conversion Systems", Proceedings of the International Renewable and Sustainable Energy Conference, Tangier, Morocco, 4-7 December 2017.

[2] M. Nadour, A. Essadki, M. Fdaili, T. Nasser, "Advanced Backstepping Control of a Wind Energy Conversion System Using a Doubly-Fed Induction Generator", Proceedings of the International Renewable and Sustainable Energy Conference, Tangier, Morocco, 4-7 December 2017.

[3] R. Chakib, A. Essadki, M. Cherkaoui, "Modeling and control of a wind system based on a DFIG by active disturbance rejection control", International review on modelling and simulations, Vol. 7, No. 4, 2014, pp. 626-637.

[4] A. Boukhris, "Robust Control by ADRC of The Wind Turbine Based on The Double Fed Induction Generator", Ph.D. Thesis, 2015.

[5] M. Smaili, "Modeling and Control of a Double Fed induction Generator for Simulation of Cogeneration Problems", Master thesis, 2013.

[6] I. Kharchouf, A. Essadki, T.Nasser, "Wind System Based on a Doubly Fed Induction Generator: Contribution to the Study of Electrical Energy Quality and Continuity of Service in the Voltage Dips Event", International Journal of Renewable Energy Research, Vol.7, No.4, 2017.

[7] J. Lopez, E. Gubia, E. Olea, J. Ruiz, L. Marroyo, "Ride through of wind turbines with doubly fed induction generator under symmetrical voltage dips", IEEE Transactions on Industrial Electronics, Vol. 56, No. 10, 2009, pp. 4246-4254.

[8] A. Lazrak, A. Abbou, "An Improved Control Strategy of DFIG Wind Turbine of Ride-Through Voltage Dips", Proceedings of the 6th International Renewable and Sustainable Energy Conference, Rabat, Morocco, 5-8 December 2018.

[9] L. Zhou, J. Liu, F. Liu, "Design and implementation of STATCOM combined with series dynamic breaking resistor for low voltage ride through of wind farms", Proceedings of the IEEE Energy Conversion

Congress and Exposition, Atlanta, GA, USA, 12-16 September 2010, pp. 2501-2506.

[10] M. S. El-Moursi, B. Bak-Jensen, M. Abdel-Rahman,."Novel STAT COM controller for mitigating SSR and damping power system oscillations in a series compensated wind park", IEEE Transactions on Power Electronics, Vol. 25, No. 2, 2009, pp. 429-441.

[11] M. Saleem, K. Y. Choi, R. Y. Kim, "Resonance damping for an LCL filter type grid-connected inverter with active disturbance rejection control under grid impedance uncertainty", Electrical Power and Energy Systems, Vol. 109, 2019, pp. 444-454.

[12] M. Saleem, B. S. Ko, S. H. Kim, S. Kim, B. S. Chowdhry, R. Y. Kim, "Active Disturbance Rejection Control Scheme for Reducing Mutual Current and Harmonics in Multi-Parallel Grid-Connected Inverters", Energies, Vol. 12, 2019, p. 4363.

[13] M. Saleem, M. H. A. K. Khushik, H. Tahir, R.Y. Kim, "Robust L Approximation of an LCL Filter Type Grid-Connected Inverter Using Active Disturbance Rejection Control under Grid Impedance Uncertainty", Energies, Vol. 14, 2021, p. 5276.

[14] S. El Aimani. "Towards a Practical Identification of a DFIG Based Wind Generator Model for Grid Assessment", Energy Procedia, Vol. 14, 2012, pp. 1677-1683.

[15] N. Elmouhi, A. Essadki, H. Elaimani, R. Chakib, "Participation of a DFIG Based Wind Energy Conversion System in Frequency Control", Proceedings of the 5th International Conference on Renewable Energies for Developing Countries, Marrakech, Morocco, 29-30 June 2020.

[16] S. Mensou, A. Essadki, I. Minka, T. Nasser, B. Bououlid Idrissi."Backstepping Controller for a Variable Wind Speed Energy Conversion System Based on a DFIG", Proceedings of the International Renewable and Sustainable Energy Conference, Tangier, Morocco, 4-7 December 2017.

[17] N. El Mouhi, A. Essadki. "Active and Reactive Power Control of DFIG used in WECS using PI Controller and Backstepping", Proceedings of the International Renewable and Sustainable Energy Conference, Tangier, Morocco, 4-7 December 2017.

[18] H. Elaimani, A. Essadki, N. Elmouhi, R. Chakib, "The Modified Sliding Mode Control of a Doubly Fed Induction Generator for Wind Energy Conversion During a Voltage Dip", Proceedings of the International Conference on Wireless Technologies, Embedded and Intelligent Systems, Fez, Morocco, 3-4 April 2019.

[19] S. El Aimani, B. François, B. Robyns, E. De Jaeger, "Dynamic Behaviour of Two Stator Flux Control Systems of a Doubly Fed Induction Generator-Based Grid-Connected Wind Turbine During Voltage Dips", Proceedings of the International Conference on Electricity Distribution Turin, Italy, 6-9 June 2005.

[20] H Elaimani, A Essadki, N Elmouhi, R Chakib, "Comparative Study of the Grid Side Converter's Control during a Voltage Dip", Journal of Energy 2020, Vol. 2020, 7892680, 11 pages.

[21] A. Boukhriss, T. Nasser, A. Essadki, A. Boualouch. "Active Disturbance Rejection Control for DFIG Based Wind Farms Under Unbalanced Grid Voltage", International Review on Modelling and Simulations, Vol. 7, No. 1, 2014.

[22] L. Xu, "Coordinated Control of DFIG's Rotor and GridSide Converters During Network Unbalance", IEEE Transactions on Power Electronics, Vol. 23, No. 3, 2008, pp. 1041-1049.

[23] A. Radaideh, M. Bodoor, A. Al-Quraan, "Active and Reactive Power Control for Wind Turbines Based DFIG Using LQR Controller with Optimal Gain-Scheduling", Journal of Electrical and Computer Engineering, Vol. 2021, 1218236.

[24] A. Boukhriss, A. Essadki, A. Bouallouch, T. Nasser, "Maximization of generated power from wind energy conversion systems using a doubly fed induction generator with active disturbance rejection control ", Second World Conference on Complex Systems, Agadir, Morocco, 10-12 November 2014.

[25] R. Rouabhi, "Control of the powers generated by a variable speed wind power system based on a doubly fed induction generator", PhD thesis, University of Batna, Faculty of Technology 2016.

[26] I. Minka, A. Essadki, S. Mensou, T. Nasser, "Power Control of a DFIG Driving by Wind Turbine: Com-

parison Study Between ADRC and PI Controller", Proceedings of the International Renewable and Sustainable Energy Conference, Tangier, Morocco, 4-7 December 2017.

[27] R. Chakib, A. Essadki, M. Cherkaoui, "Modeling and control of a wind system based on a DFIG by active disturbance rejection control", International review on modelling and simulations, Vol. 7, No. 4, 2014, pp. 626-637.

[28] A. G. Abo-Khalil, W. Alharbi, A. Al-Qawasmi, M. Alobaid, I. Alarifi, "Modeling and control of unbalanced and distorted grid voltage of grid-connected DFIG wind turbine", International Transactions on Electrical Energy Systems, Vol. 31, No. 5, 2021.

[29] S. Mensou, A. Essadki, T. Nasser, B. Bououlid Idrissi, "A direct power control of a DFIG basedWECS during symmetrical voltage dips", Protection and Control of Modern Power Systems, Vol. 5, No. 5, 2020.

[30] L. Xu, "Dynamic Modeling and Control of DFIG-BasedWindTurbines Under Unbalanced Network Conditions", IEEE Transactions on Power Systems, Vol. 22, No. 1, 2007, pp.314-323.

[31] M.B.C Salles, A.J.S Filho and A.P.Grilo, "A Study on the Rotor Side Control of DFIG-based Wind turbine during Voltage Sags without Crowbar System" Proceedings of the International Conference on Renewable Energy Research and Applications, Nagasaki, Japan, 11-14 November 2012.

[32] A. Cheriet, A. Bekri, H. Gouabi, A. Hamed, "Nonlinear backstepping control optimized by genetic algorithm for the control of a wind turbine" International Journal of Industrial Electronics and Electrical Engineering, Vol. 7, No. 6, 2019, pp. 3-7.

[33] A. Boulmane, Y. Zidani, D. Belkhayat, and M. Bouchouirbat, "A GA-based adaptive mechanism for sensorless vector control of induction motor drives for urban electric vehicles", Turkish Journal of Electrical Engineering & Computer Sciences, Vol. 28, No. 3, 2020, pp. 1731-1746.

[34] K. E. Okedu, M. Al Tobi, S. Al Araimi, "Comparative Study of the Effects of Machine Parameters on DFIG and PMSG Variable Speed Wind Turbines During Grid Fault", Frontiers in Energy Research, 2021.